

RESEARCH

Open Access



Transforming growth factor beta1 targets estrogen receptor signaling in bronchial epithelial cells

L. Cody Smith^{1,2}, Santiago Moreno², Lauren Robertson^{2,3}, Sarah Robinson^{2,3}, Kristal Gant^{2,3}, Andrew J. Bryant⁴ and Tara Sabo-Attwood^{2,3*} 

Abstract

Background: Sex differences in idiopathic pulmonary fibrosis (IPF) suggest a protective role for estrogen (E2); however, mechanistic studies in animal models have produced mixed results. Reports using cell lines have investigated molecular interactions between transforming growth factor beta1 (TGF- β 1) and estrogen receptor (ESR) pathways in breast, prostate, and skin cells, but no such interactions have been described in human lung cells. To address this gap in the literature, we investigated a role for E2 in modulating TGF- β 1-induced signaling mechanisms and identified novel pathways impacted by estrogen in bronchial epithelial cells.

Methods: We investigated a role for E2 in modulating TGF- β 1-induced epithelial to mesenchymal transition (EMT) in bronchial epithelial cells (BEAS-2Bs) and characterized the effect of TGF- β 1 on ESR mRNA and protein expression in BEAS-2Bs. We also quantified mRNA expression of ESRs in lung tissue from individuals with IPF and identified potential downstream targets of E2 signaling in BEAS-2Bs using RNA-Seq and gene set enrichment analysis.

Results: E2 negligibly modulated TGF- β 1-induced EMT; however, we report the novel observation that TGF- β 1 repressed ESR expression, most notably estrogen receptor alpha (ESR1). Results of the RNA-Seq analysis showed that TGF- β 1 and E2 inversely modulated the expression of several genes involved in processes such as extracellular matrix (ECM) turnover, airway smooth muscle cell contraction, and calcium flux regulation. We also report that E2 specifically modulated the expression of genes involved in chromatin remodeling pathways and that this regulation was absent in the presence of TGF- β 1.

Conclusions: Collectively, these results suggest that E2 influences unexplored pathways that may be relevant to pulmonary disease and highlights potential roles for E2 in the lung that may contribute to sex-specific differences.

Keywords: Transforming growth factor beta1, Estrogen, Estrogen receptor, Lung, Fibrosis

Background

Epidemiological studies have associated sex with idiopathic pulmonary fibrosis (IPF) where males are more negatively impacted and females have better survival rates [1–5]. In addition, a study by our group found a statistical interaction between sex and IPF severity based on gene expression in diseased lung tissue [6]. Based on

these observations, several hypotheses suggest a role for estrogens and androgens.

Sex-based studies of pulmonary fibrosis in small animal models have produced mixed results. Several reports suggest that estrogen (E2) is protective and androgens exacerbate fibrotic responses. For example, bleomycin caused increased pulmonary fibrosis in male mice compared to females [7, 8], and a recent study found that it was the presence of the Y chromosome and not necessarily sex itself that predisposed the lung to increased bleomycin-induced fibrosis in male and female mice [9]. Conversely, a study in rats indicated that females exhibited increased pulmonary fibrosis in response to bleomycin compared to males [10]. Importantly,

* Correspondence: sabo@phhp.ufl.edu

²Center for Environmental and Human Toxicology, University of Florida, Gainesville, FL, USA

³Department of Environmental and Global Health, Center for Environmental and Human Toxicology, University of Florida, Box 110885, 2187 Mowry Rd, Gainesville, FL 32611, USA

Full list of author information is available at the end of the article



variable responses to bleomycin in mice may be due to differential activity of bleomycin hydrolase between male and females [11]. Conversely, E2 was protective in ovariectomized mice where a significant increase in total lung collagen content and airway subepithelial collagen deposition was observed in ovariectomized mice which was mitigated by E2 administration [12].

Current reports have not probed the molecular mechanisms impacted by hormones in the lung contributing to sex-based differences in fibrotic disease except one study which found increased TGF- β 1 expression in rat fibroblasts exposed to E2 [10]. Regulation of TGF- β 1 by E2 has been extensively characterized in other model systems and the effects appear to be contextual. For example, E2 inhibited TGF- β 1 signaling in breast cancer cells by reducing the expression of activators of TGF- β 1 [13] and by increasing degradation of SMAD proteins [14, 15]. Conversely, E2 increased TGF- β 1 secretion in dermal fibroblasts [16], and TGF- β 1 levels were reduced in the kidneys of diabetic female mice lacking estrogen receptor alpha (ESR1) compared to wildtype mice suggesting positive regulation of TGF- β 1 by E2 [17].

E2 binds and activates several receptors including the nuclear transcription factors estrogen receptor alpha (ESR1), estrogen receptor beta (ESR2), and several variants thereof, and the putative membrane-bound G-protein coupled estrogen receptor 1 (GPER1). Studies aiming to decipher receptor-specific effects on TGF- β 1 signaling have been limited to non-lung cells and tissues (i.e. breast). For example, Stope et al. found that ESR1 but not ESR2 inhibited TGF- β 1 activation in breast cancer cells [18] while others found that both ESR1 and ESR2 suppressed TGF- β 1 signaling by associating with and acting as a transcriptional corepressor for SMAD3 [19, 20]. Other studies showed a role for GPER1 in mediating E2-dependent reduction in SMAD protein activation in breast cancer cells [21] and TGF- β 1-induced extracellular matrix (ECM) production in human and rat mesangial cells [22].

Given the preponderance of opposing actions of E2 on TGF- β 1 in *in vitro* systems other than the lung and the epidemiological evidence suggesting a male sex-bias in IPF, we hypothesized that E2 would inhibit TGF- β 1-induced signaling in lung epithelial cells. To test this hypothesis, we investigated the impact of E2 on TGF- β 1-induced epithelial to mesenchymal transition (EMT), characterized the expression of ESRs in bronchial epithelial cells and lung tissue from individuals with IPF, and performed RNA-Seq analysis to identify targets of E2 in bronchial epithelial cells.

Methods

Chemicals

Recombinant human transforming growth factor beta1 (TGF- β 1) was purchased from R&D Systems (> 97% purity, Catalog No. 240-B002, Minneapolis, MN) and 17 β -Estradiol

(E2) was purchased from Sigma (\geq 98% purity, Catalog No. E2758, Saint Louis, MO).

Human lung samples

The human lung tissue samples used in this study were a kind gift from Dr. Andrew Bryant. The explanted lung tissue was obtained from subjects undergoing lung transplant for IPF and from lungs rejected for transplant from normal controls per the National Institutes of Health Lung Tissue Research Consortium (protocol no. 14-99-0011). This study consisted of fifteen patients, eight with IPF ($n = 8$) and seven controls ($n = 7$) described in detail in Table 1. A diagnosis of IPF was determined based on ATS criteria [23, 24]. The protocol for collection of lung tissue samples and subsequent studies were approved by the institutional review board at Vanderbilt University and the University of Florida [25]. Immediately after lung biopsy or resection, a portion of the lung was removed and flash-frozen in liquid nitrogen or dry ice and stored at -80°C .

Cell culture

Human bronchial epithelial cells (BEAS-2Bs, CRL-9609[™]) were purchased from ATCC and cultured according to manufacturer's specifications. STR analysis and mycoplasma contamination testing was not performed. Cells were cultured in bronchial epithelial growth medium (BEGM) consisting of bronchial epithelial basal medium (BEBM, Lonza CC-3171, Walkersville, MD) and the BEGM SingleQuot Kit Supplements & Growth Factors (Lonza CC-4175) but exchanging gentamicin for Penicillin-Streptomycin-Neomycin (PSN) Antibiotic Mixture (Gibco 15,640, ThermoFisher Scientific Inc., Waltham, MA). Cells were cultured in T75 Corning[™] U-Shaped Cell Culture Flasks (Corning 430,641 U, Fisher Scientific Co LLC, Pittsburgh, PA) coated with a matrix (4.5 mL per 75 cm²) consisting of 0.01 mg/mL fibronectin (Akron AK8350, City, State), 0.03 mg/mL bovine collagen (Gibco A10644-01), and 0.01 mg/mL BSA (Fisher BP1605) in BEBM. Cells were sub-cultured up to 11 times before use in exposure studies. All exposures were performed in BEGM without the supplied bovine pituitary extract (BPE) aliquot because its composition is not defined. For the gene expression experiments, BEAS-2Bs were plated at 40,000 cells/mL on matrix-coated 12-well Nunc[™]

Table 1 Patient demographic data

Characteristics	Controls	Patients
Male/Female	2/3	8/0
Age ^a	64 \pm 14.78	61.5 \pm 7.11
Smoking Status		
Never	4	6
Ever	1	2
FVC, % predicted ^a	105.2 \pm 7.79	42.9 \pm 14.39

^aMean \pm SD

Cell-Culture-Treated Multidishes (ThermoFisher Scientific Inc.), allowed to adhere overnight, and subsequently exposed for 48 h to the indicated concentrations of TGF- β 1 dissolved in 0.1% BSA (Fisher BP1605) and 4 mM HCl or 10 nM E2 dissolved in DMSO (Mediatech Inc. MT25950CQC). Doses of TGF- β 1 and E2 were chosen based on efficacy in previous experiments [26–30]. For the protein expression experiments, BEAS-2Bs were plated at 60,000 cells/mL on matrix-coated 6-well Corning® Costar® cell culture plates (Costar 3516), allowed to adhere overnight, and subsequently exposed for 48 h to the indicated concentrations of TGF- β 1 in BEBM without BPE. All chemical solvent concentrations were maintained below 0.1%.

Total RNA extraction and purification

Frozen whole lung samples were pulverized over liquid nitrogen using a mortar and pestle then mechanically disrupted in RNA STAT-60™ Reagent (Tel-Test, Inc. Cs-502, Friendswood, TX) using a handheld homogenizer, and cell lysates were collected in RNA STAT-60™ Reagent and vortexed to promote lysis. RNA was extracted per manufacturer's specifications followed by overnight precipitation at -20°C using 100% molecular biology grade isopropanol (Fisher BioReagents™ BP26184) containing 0.067% v/v GlycoBlue™ Coprecipitant (Ambion® AM9515). Precipitated RNA was pelleted by centrifugation at 14000 x g for 45 min at 4°C and purified by washing 2X with 75% molecular biology grade absolute ethanol (Fisher BioReagents™ BP28184). RNA pellets were reconstituted in 15 μL RNase-secure™ (Ambion® AM7010). RNA was quantified using a Synergy™ H1 plate reader (BioTek Instrument, Inc., Winooksi, VT) and RNA integrity was analyzed using a Bioanalyzer 2100 instrument (Agilent Technologies, Santa Clara, CA).

qPCR

RNA (1–2 μg) was DNase-treated using the PerfeCTa DNase I Kit (Quanta BioSciences 95,150-01 k, VWR International LLC, Suwanee, GA) and subsequently reverse transcribed using the qScript™ cDNA Synthesis Kit (Quanta BioSciences 95,047). cDNA was diluted 1:20 in RNase-DNase free water. Each 10 μL qPCR reaction contained 1 \times SsoAdvanced™ Universal SYBR® Green Supermix (Bio-Rad 172–5270, Hercules, CA), 850 nM forward and reverse primers, and 3.3 μL of the cDNA dilution. Per MIQE guidelines [31], gene specific primers and cycling parameters are displayed in Table 2. *ESR2* primers were purchased from Bio-Rad (Unique Assay ID: qHsaCID0013184). Each qPCR reaction was followed by melt curve analysis to verify primer specificity. Cq values were determined by regression method using the CFX Manager 2.1 software and quantified using the relative $\Delta\Delta\text{Cq}$ method [32] or the ratio method [33] when indicated. In the case of no amplification, a Cq value of

40 was applied. For the cell culture experiments, target gene expression was normalized to glyceraldehyde 3-phosphate dehydrogenase (*GAPDH*) expression and to ribosomal protein S13 (*RPS13*) expression in the human lung tissue samples.

Protein extraction and purification

After exposure, media was removed, and cells were washed 3X with ice-cold PBS and subsequently collected in 200 μL RIPA Lysis and Extraction Buffer (Pierce Biotechnology 89,900) containing Pierce™ Protease Inhibitor Tablets (Pierce Biotechnology 88,265) using a cell scraper. The lysates were passed 5X through a 25-gauge needle and incubated on ice for 30 min with intermittent mixing. Thereafter, the lysates were centrifuged at 14000 x g for 20 min at 4°C , supernatants were removed, and total protein quantified using the Pierce BCA Protein Assay Kit (Pierce Biotechnology 23,225).

Western blot

For SDS-PAGE, total protein (15 μg) was diluted in Novex™ Tris-Glycine SDS Sample Buffer (2X) (Invitrogen LC2676) and loaded onto a Novex™ WedgeWell™ 4–12% Tris-Glycine Mini Gel (Invitrogen XP04120BOX). Electrophoresis was performed for 30 min at 225 V and electrophoresed proteins were subsequently transferred to nitrocellulose membranes (GVS Life Sciences EP4HY00010) by semi-dry transfer method under 15 V for 30 min. Blots were blocked with 5% dehydrated milk dissolved in TBST for 1 h at room temperature, then incubated with mouse monoclonal antibody specific for estrogen receptor α (anti-ESR1, Santa Cruz Biotechnology, Inc. SC-514857, Dallas, TX) diluted 1:100 in blocking solution overnight at 4°C . Blots were washed 3X in TBST for 10 min and incubated with HRP-linked Rabbit anti-Mouse IgG (H + L) Secondary Antibody (Pierce 31,450, Rockford, IL) diluted 1:4000 in TBST for 1 h at room temperature. Blots were washed 3X with TBST for 10 min at room temperature, then 1X with TBS at room temperature. Thereafter, blots were incubated with 1:1 solution of Clarity™ Western ECL Blotting Substrates (Bio-Rad 170–5060, Hercules, CA) and imaged using the auto-exposure option on a Bio-Rad ChemiDoc™ MP system (Bio-Rad 17,001,402). After probing with anti-ESR1, blots were incubated 2X for 10 min at room temperature in mild stripping buffer (0.1 M Glycine, 20 mM MgAcetate, 50 mM KCl, pH 2.2), then washed 3X with TBST for 5 min at room temperature. To verify antibody stripping, the blot was probed with HRP-linked secondary antibody and re-imaged as before. After verification of anti-ESR1 removal, the blot was incubated in blocking solution for 1 h at room temperature, then incubated with mouse monoclonal antibody specific for β -Actin (anti- β -Actin, Sigma A5441) diluted 1:5000 in blocking

Table 2 Primer information for qPCR

Gene	Forward (5'-3')	Reverse (5'-3')	Protocol	Efficiency	Source
<i>GAPDH</i>	GAAGGTGAAGGTCGGAGTC	GAAGATGGTATGGGATTTTC	95C 3m; 95C 10s, 60C 30s, x40	93.9%	[92]
<i>ESR1</i>	CCACCAACCAGTGCACCATT	GGTCTTTTCGTATCCCACCTTTC	95C 3m; 95C 10s, 60C 30s, x40	100.7%	[93]
<i>ESR2</i>	Proprietary	Proprietary	95C 3m; 95C 10s, 60C 30s, x40	102.9%	Bio-Rad
<i>GPER</i>	GCTCCCTGCAAGCAGTCTTT	GAAGGTCCTCCCGAGAAAGC	95C 3m; 95C 10s, 60C 30s, x40	97.2%	[94]
<i>SNAI1</i>	CCAGACCCACTCAGATGTCAA	GGACTCTTGGTGCTTGGA	95C 3m; 95C 10s, 58C 30s, x40	97.2%	[94]
<i>CDH1</i>	GAAAGCGGCTGATACTGACC	CTCAGACTAGCAGCTTCGGA	95C 3m; 95C 10s, 58C 30s, x40	104.9%	[94]
<i>ACTA2</i>	CATCATGCGTCTGGATCTGG	GGACAATCTCACGCTCAGCA	95C 3m; 95C 10s, 60C 30s, x40	94.8%	[95]
<i>MMP2</i>	TGTGTTCTTTGCAGGGAATG	TCCAGAAATTTGTCTCCAGCA	95C 3m; 95C 10s, 58C 30s, x40	93.6%	[96]
<i>CTGF</i>	AATGCTGCGAGAGTGGGT	CGGCTCTAATCATAGTTGGGTCT	95C 3m; 95C 10s, 60C 30s, x40	96.4%	[97]
<i>VIM</i>	GCGTGAAATGGAAGAGAACT	GGTATCAACCAGAGGGAGTG	95C 3m; 95C 10s, 56C 10s, 72C 30s, x40	104.0%	[30]
<i>MUC15</i>	CCATCGGCGACTTTATGACG	TCTTCACTTCTGGCATGGCT	95C 3m; 95C 10s, 60C 30s, x40	92.1%	[94]

solution overnight at 4 °C. The blot was subsequently washed as before, incubated in HRP-linked Rabbit anti-Mouse IgG (H + L) Secondary Antibody (Pierce 31,450) diluted 1:5000 in TBST for 1 h at room temperature, and imaged as before. Densitometry was performed in ImageJ [34] using the Gel Analysis method outlined in the ImageJ documentation.

RNA-Seq library preparation and sequencing

RNA library construction was performed at the Interdisciplinary Center for Biotechnology Research (ICBR) Gene Expression Core, University of Florida (UF). RNA concentration was determined on Qubit® 2.0 Fluorometer (ThermoFisher/Invitrogen, Grand Island, NY), RNA quality was assessed using the Agilent 2100 Bioanalyzer. Total RNA with 28S/18S > 1 and RNA integrity number (RIN) ≥ 7 was used for RNA-seq library construction. The RINs of all total RNA samples were 9.7–10. 2 µL of 1:2000 diluted External RNA Controls Consortium (ERCC) Spike-In Mix (Ambion™ 4,456,740, ThermoFisher Scientific Inc.) was added to 100 ng of high-quality total RNA followed by mRNA isolation using NEBNext Poly(A) mRNA Magnetic Isolation module (New England Biolabs E7490, Ipswich, MA) and RNA library construction with NEBNext Ultra RNA Library Prep Kit for Illumina (New England Biolabs E7530) according to the manufacturer's user guide. Specifically, 100 ng of total RNA together with 2 µL of 1:2000 diluted ERCC was added to extracted mRNA with 15 µL of NEBNext Magnetic Oligo d(T)25 and fragmented in NEBNext First Strand Synthesis Buffer by heating at 94 °C for 8 min, followed by first-strand cDNA synthesis using reverse transcriptase and random primers. Synthesis of ds cDNA was done using the 2nd strand master mix provided in the kit. The resulting double-stranded cDNA was end-repaired, dA-tailed and ligated with NEBNext adaptors. Finally, library was enriched by 13 cycles of amplification, and purified by Meg-Bind RxnPure Plus beads (Omega Biotek M1386, Norcross, GA). Bar-coded libraries

were sized on the bioanalyzer, quantitated by QUBIT and qPCR (Kapa Biosystems KK4824, Wilmington, MA). Seventeen individual libraries were pooled at equal molar (20 nM).

Bar-coded cDNA was sequenced using the 2 × 100 configuration in 2 lanes of a HiSeq 3000 instrument (Illumina, San Diego, CA). The yield for the run was in the expected range, the quality was good with Q30 > 96.25%, and the pool was well-balanced (in terms of number of reads per samples).

Bioinformatics

Short reads were trimmed and filtered to remove low-quality reads using Trimmomatic version 0.36. Quality control was assessed using the FastQC tool, version 0.11.4. Short reads were aligned to the transcriptome using STAR version 2.5.2a. Transcript quantification and differential analysis was performed using RSEM version 1.2.31. Differential analysis was performed at the level of coding genes, all transcript, and all splicing isoforms. Coding genes, transcripts, and splicing isoforms were considered statistically significant if FDR-corrected *p*-value ≤ 5% and fold change > 1.5 in either direction. Clustering analysis was performed using the 'gplots' package in R version 3.3.2 (2016-10-31). Gene set enrichment analysis was performed using Pathway Studio® Version 11.4.0.8 operating on the ResNet Mammalian database (Elsevier). Statistically significant enrichment (*p* ≤ 0.05) of predefined gene sets was determined by Mann-Whitney U-test. The data discussed in this publication have been deposited in NCBI's Gene Expression Omnibus [35] and are accessible through GEO Series accession number GSE100574 (<https://www.ncbi.nlm.nih.gov/geo/query/acc.cgi?acc=GSE100574>).

Statistics

Normality of experimental data was determined by D'Agostino & Pearson omnibus normality test, Shapiro-Wilk normality test, or KS normality test using

GraphPad Prism software (Version 5.01, GraphPad Software, Inc.). Data were determined to be normal by passing at least one normality test ($p < 0.05$). For qPCR and western blot analyses, statistically significant differences ($p < 0.05$) in mean fold changes between experimental groups were determined by one-way ANOVA followed by Newman-Keuls multiple comparison test or unpaired, two-tailed t test when indicated using GraphPad Prism software. If the data were not normal, statistically significant differences were determined by two-tailed Mann-Whitney U test.

Results

TGF- β 1 induces changes consistent with EMT

To begin investigations, we optimized a well-characterized model of TGF- β 1-induced EMT based on changes in gene expression. BEAS-2Bs were exposed to TGF- β 1 (0.1, 1, and 5 ng/mL) for 48 h and mRNA expression of molecular markers for EMT were assayed by qPCR. Results revealed a dose-dependent response where exposure of cells for 48 h to 1 and 5 ng/mL TGF- β 1 caused a significant reduction in expression of the epithelial cell type marker, E-cadherin (*CDH1*), compared to control cells (Fig. 1a). Conversely, exposure of cells to 1 and 5 ng/mL TGF- β 1 caused a significant increase in expression of the mesenchymal cell type markers, Vimentin (*VIM*), Snail family transcriptional repressor 1 (*SNAI1*), N-cadherin (*CDH2*), and Fibronectin (*FNI*) compared to control cells (Fig. 1b, d-f). Exposure of cells to TGF- β 1 did not affect expression of the myofibroblast cell type marker, alpha smooth muscle actin (*ACTA2*) at any tested doses (Fig. 1c).

E2 does not significantly affect TGF- β 1-induced EMT

A role for E2 in modulating TGF- β 1-induced EMT was assessed by exposing BEAS-2B cells to 5 ng/mL TGF- β 1 in the presence and absence of 10 nM E2 for 48 h. Thereafter, expression of EMT marker genes was assayed by qPCR. As expected, 5 ng/mL TGF- β 1 caused a reduction (0.686-fold, $p > 0.05$) in *CDH1* mRNA expression (Fig. 2a). However, the addition of 10 nM E2 did not significantly affect the TGF- β 1-induced response or *CDH1* expression individually (Fig. 2a). Exposure of cells to 5 ng/mL TGF- β 1 caused a trend of increased mRNA expression of the mesenchymal markers, *VIM* ($p > 0.05$), *SNAI1* ($p > 0.05$), *CDH2*, *FNI* (Fig. 2b, d-f) and similar to *CDH1*, exposure of cells to 5 ng/mL TGF- β 1 in the presence of 10 nM E2 did not result in a statistically significant difference from cells exposed to TGF- β 1 individually (Fig. 2b, d-f). As before, there were no statistically significant differences in expression of *ACTA2* compared to control cells in any exposure group, however there was a 1.74-fold trend of increased expression in the co-exposure group (Fig. 2c). Statistically significant differences could not be determined

between groups for *CDH2* and *FNI* because these data were generated from only two independent experiments.

TGF- β 1 reduces estrogen receptor mRNA and protein expression

Next, we investigated whether estrogen receptor mRNA expression was a target for TGF- β 1. The baseline expression levels of estrogen receptor alpha (*ESR1*), estrogen receptor beta (*ESR2*), and g-protein coupled estrogen receptor (*GPER1*) in control cells were expressed as a ratio to *ESR1* based on the method described by Pfaffl et al. [33] to determine relative baseline expression levels. The relative expression of each receptor subtype was *GPER1* > *ESR1* > *ESR2* (Fig. 3a). Exposing BEAS-2Bs to increasing concentrations of TGF- β 1 (0.1, 1, and 5 ng/mL) for 48 h caused a 1.81-, 3.11-, and 2.87-fold ($p < 0.05$) decrease in *ESR1* mRNA expression compared to controls (Fig. 3b). Similar trends were observed for *ESR2* mRNA expression compared to controls (Fig. 3c), and a 1.44, 1.72, and 1.78-fold ($p < 0.05$) decrease in *GPER1* mRNA expression compared to controls (Fig. 3d) was observed for the three doses, respectively.

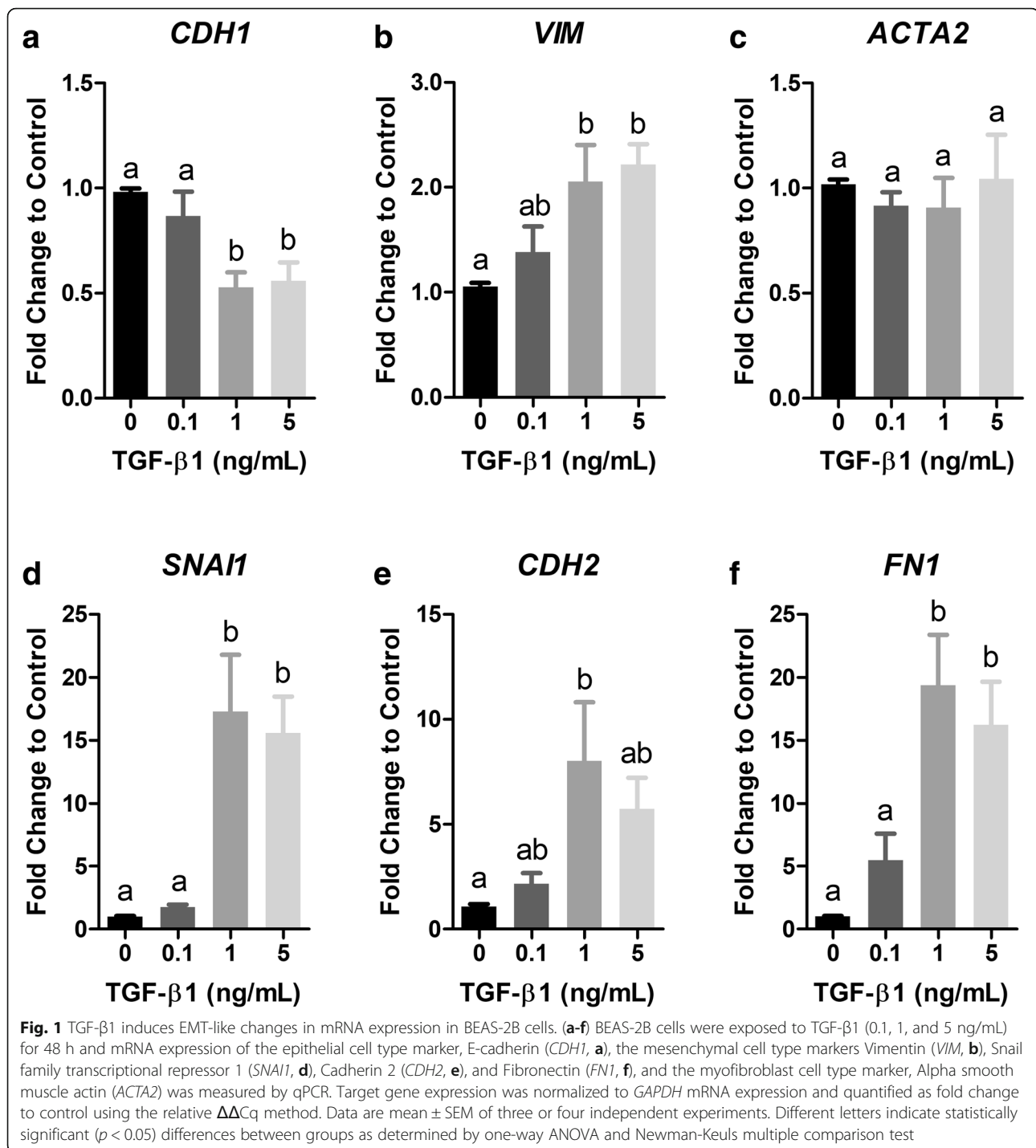
BEAS-2Bs were exposed to TGF- β 1 (0.1, 1, and 5 ng/mL) for 48 h and ESR1 was detected by western blot to determine if TGF- β 1 reduced ESR1 protein levels (Fig. 4a). Signal intensity was quantified by densitometry using ImageJ (Fig. 4b). Similar to the mRNA results, TGF- β 1 (0.1, 1, and 5 ng/mL) caused a 2.09-, 2.77-, and 3.76-fold significant decrease in ESR1 protein levels, respectively (Fig. 4b).

Estrogen receptor mRNA expression is reduced in lungs of patients with IPF

We next questioned whether our in vitro results translated in vivo. To answer this, mRNA expression of *ESR1*, *ESR2*, and *GPER1* was compared in lung tissue from healthy controls to individuals with end-stage IPF given that those with IPF tend to have higher TGF- β 1 serum levels compared to healthy controls [36]. A qPCR analysis found that *ESR1* and *GPER1* mRNA expression was significantly reduced in the lungs of patients with end-stage IPF compared to healthy controls while there was a trend of reduced expression of *ESR2* in the former group (Fig. 5a-c).

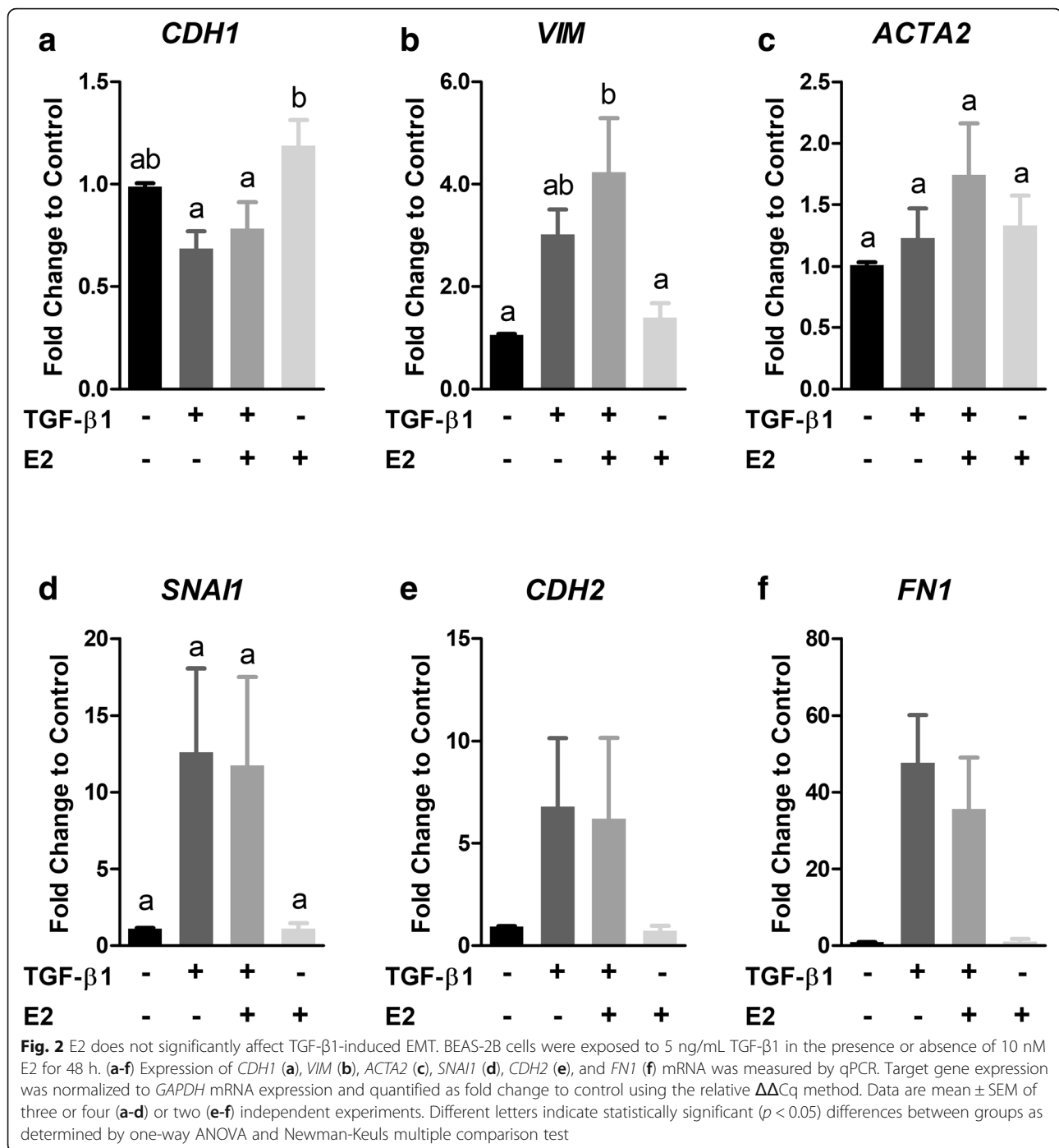
TGF- β 1 and E2 exhibit unique transcriptional profiles

RNA-Seq was performed to identify transcriptional targets of E2 in bronchial epithelial cells and cellular processes that may be affected by the observed down-regulation of ESR expression by TGF- β 1. For this experiment, BEAS-2Bs were exposed to either vehicle control, 5 ng/mL TGF- β 1 for 48 h, 10 nM E2 for 24 h, or pre-exposed to 5 ng/mL TGF- β 1 for 24 h and subsequently co-exposed to both 5 ng/mL TGF- β 1 and 10 nM



E2 for 24 h (Fig. 6a). Differential expression analysis resulted in 2182 coding genes with FDR-corrected p -value ≤ 0.05 and $\text{Log}_2(\text{Fold Change}) > |0.6|$ compared to controls in the TGF- β 1 group. The expression of 2119 coding genes was altered in the group co-exposed to TGF- β 1 and E2, and 10 in the group exposed to E2. In sum, 379, 316, and 6 genes were specifically altered in the TGF- β 1, TGF- β 1 + E2, and E2 groups, respectively,

while 1798 genes were differentially regulated in both the TGF- β 1 and TGF- β 1 + E2 groups, and 4 were differentially regulated in all groups (Fig. 6b). Many of the genes significantly up-regulated by TGF- β 1, such as CTGF, MMP2 and VIM, are well-known targets of this pathway (Fig. 7, Additional file 1: Table S1). Other genes significantly up-regulated in all treatment groups included Sprouty RTK signaling antagonist 4 (*SPRY4*) and



Dual specificity phosphatase 6 (*DUSP6*), and significantly down-regulated genes included Potassium voltage-gated channel subfamily Q member 1 (*KCNQ1*) and RAS protein activator like 1 (*RASAL1*) (Additional file 1: Tables S1-S2, Table 3). Genes that were specifically regulated by E2 included Retinol binding protein 7 [*RBP7*, $\text{Log}_2(\text{Fold Change}) = -1.65$] and Chloride intracellular channel 3 [*CLIC3*, $\text{Log}_2(\text{Fold Change}) = -0.73$] (Table 3). A hierarchical clustering analysis of genes

differentially regulated in at least one exposure group showed that the expression profiles of the TGF-β1 and TGF-β1 + E2 group were more similar to each other than to the expression profile of E2 (Fig. 6c).

The expression of genes relevant to pulmonary fibrosis and this current work was validated by qPCR in an independent experiment (Fig. 7). As expected, exposure to TGF-β1 caused a significant reduction in *ESR1* mRNA expression (Fig. 7a) and increased the expression of

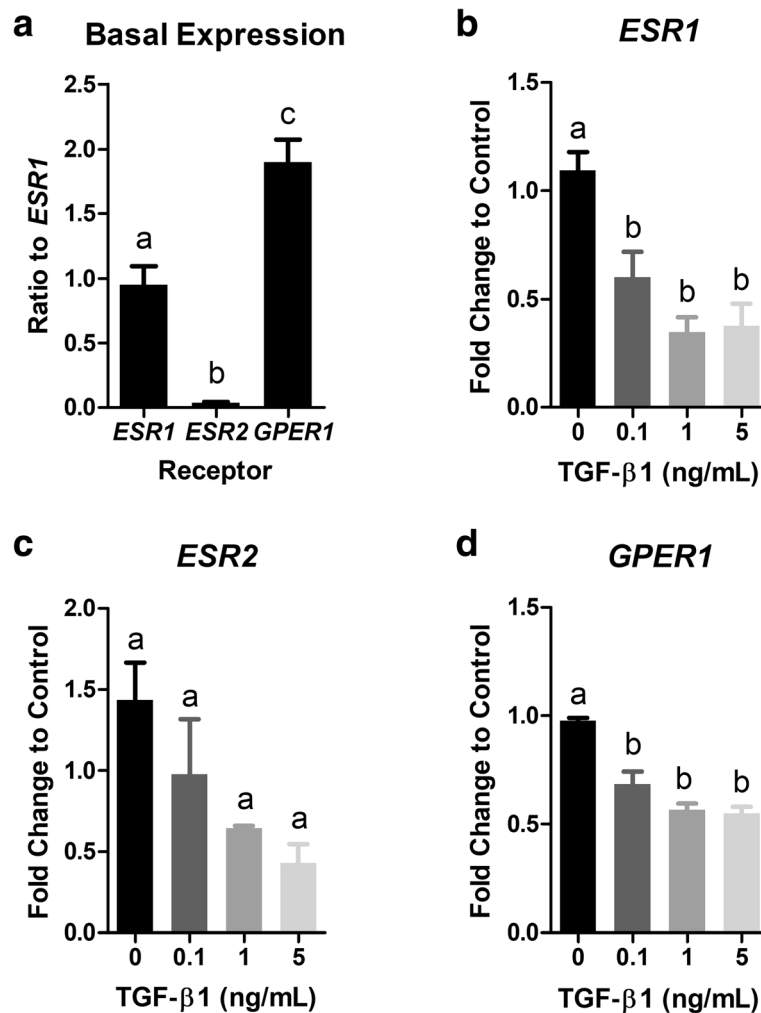


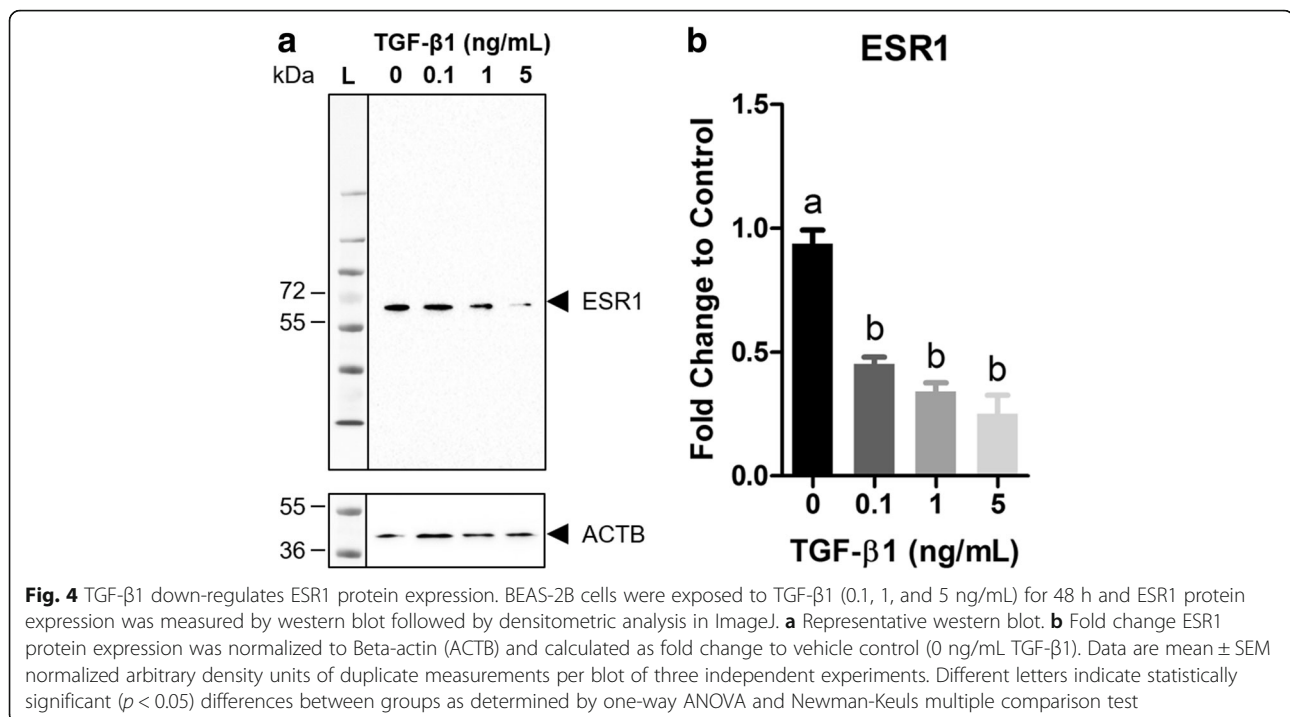
Fig. 3 TGF- β 1 down-regulates *ESR1*, *ESR2*, and *GPER1* mRNA expression in BEAS-2Bs. (a) Relative expression of estrogen receptor subtypes in control cells was $GPER1 > ESR1 > ESR2$. ESR gene expression was normalized to *GAPDH* mRNA expression and calculated as a ratio to *ESR1* mRNA expression. (b-d) BEAS-2B cells were exposed to TGF- β 1 (0.1, 1, and 5 ng/mL) for 48 h and expression of *ESR1* (n = 3; b), *ESR2* (n = 2; c), and *GPER1* (n = 3; d) mRNA was measured by qPCR. Target gene expression was normalized to *GAPDH* mRNA expression and quantified as fold change to control using the relative $\Delta\Delta Cq$ method. Data are mean \pm SEM and different letters indicate statistically significant ($p < 0.05$) differences between groups as determined by one-way ANOVA and Newman-Keuls multiple comparison test

known targets of TGF- β 1 such as Connective tissue growth factor (*CTGF*, Fig. 7b), *VIM* (Fig. 7c), and Matrix metalloproteinase 2 (*MMP2*, Fig. 7d). The presence of E2 in the co-exposure group did not have a clear effect on the expression of these genes compared to the TGF- β 1 group.

TGF- β 1 and E2 differentially regulate gene sets

Gene set enrichment analysis (GSEA) [37] was performed to identify statistical enrichment in the RNA-Seq data of curated pathways using Pathway Studio[®] Version 11.4.0.8 (Elsevier). The GSEA resulted in differential enrichment of biological function and disease pathways among the exposure groups. As expected, exposure to TGF- β 1 resulted in enrichment of pathways such as

ECM turnover and skin fibrosis (Table 4). Exposure to TGF- β 1 also resulted in statistical enrichment of pathways including alveolar epithelial cell dysfunction, Ca²⁺ flux regulation, classical and alternative complement pathways, and neutrophil chemotaxis (Table 4). In most cases, similar enrichment and median changes were observed in the co-exposure group (TGF- β 1 + E2) and the TGF- β 1 only exposure group except for alveolar epithelial cell dysfunction which was not statistically enriched in the co-exposure group (Table 4). E2 also caused enrichment of classical and alternative complement pathways, airway smooth muscle cell contraction, Ca²⁺ flux regulation, and ECM turnover, however, the median change of the latter two pathways was inverse (down-regulated) compared to the median change



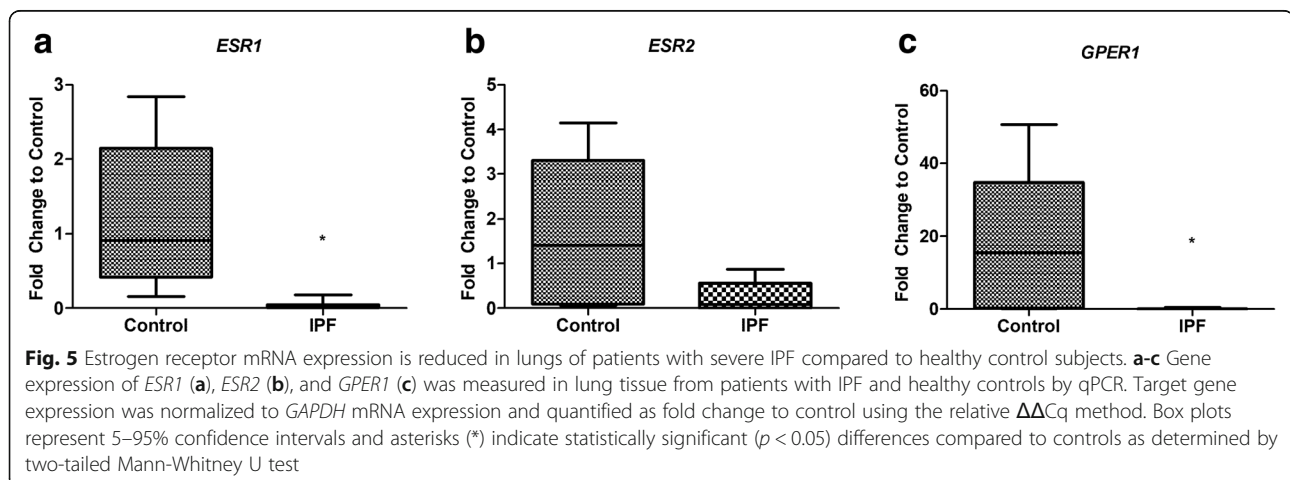
observed in the TGF- β 1 and co-exposure groups (Table 4). The ECM pathway is presented graphically to highlight the inverse regulation of genes in the pathway by TGF- β 1 (Fig. 8, top) and E2 (Fig. 8, bottom). E2 specifically caused statistical enrichment of pathways including histone acetylation and phosphorylation pathways, nucleosome-remodeling factor (NURF) in chromatin remodeling, and vasodilation activation (Table 4).

Discussion

This work was motivated by evidence suggesting hormones may influence gene regulation in the lung and contribute to sex differences in pulmonary diseases such as fibrosis. Using a well-established model lung epithelial cell

line, we investigated the impact of E2 on TGF- β 1-induced EMT. We report that although TGF- β 1-induced EMT was not significantly affected by E2, this may be due to the novel observation that TGF- β 1 repressed ESR expression, most notably ESR1. We extended this observation to identify novel targets of E2 by RNA-Seq that may be susceptible to TGF- β 1-induced repression of ESRs such as chromatin remodeling processes and ECM turnover.

We first characterized the relative expression levels of the ESRs in our model cell line. We found that *GPER1* was the most abundant followed by *ESR1* while *ESR2* was least expressed (Fig. 3a). Our results are similar to a study by Stabile et al. that found higher expression of *ESR1* than *ESR2* in human lung adenocarcinomas and



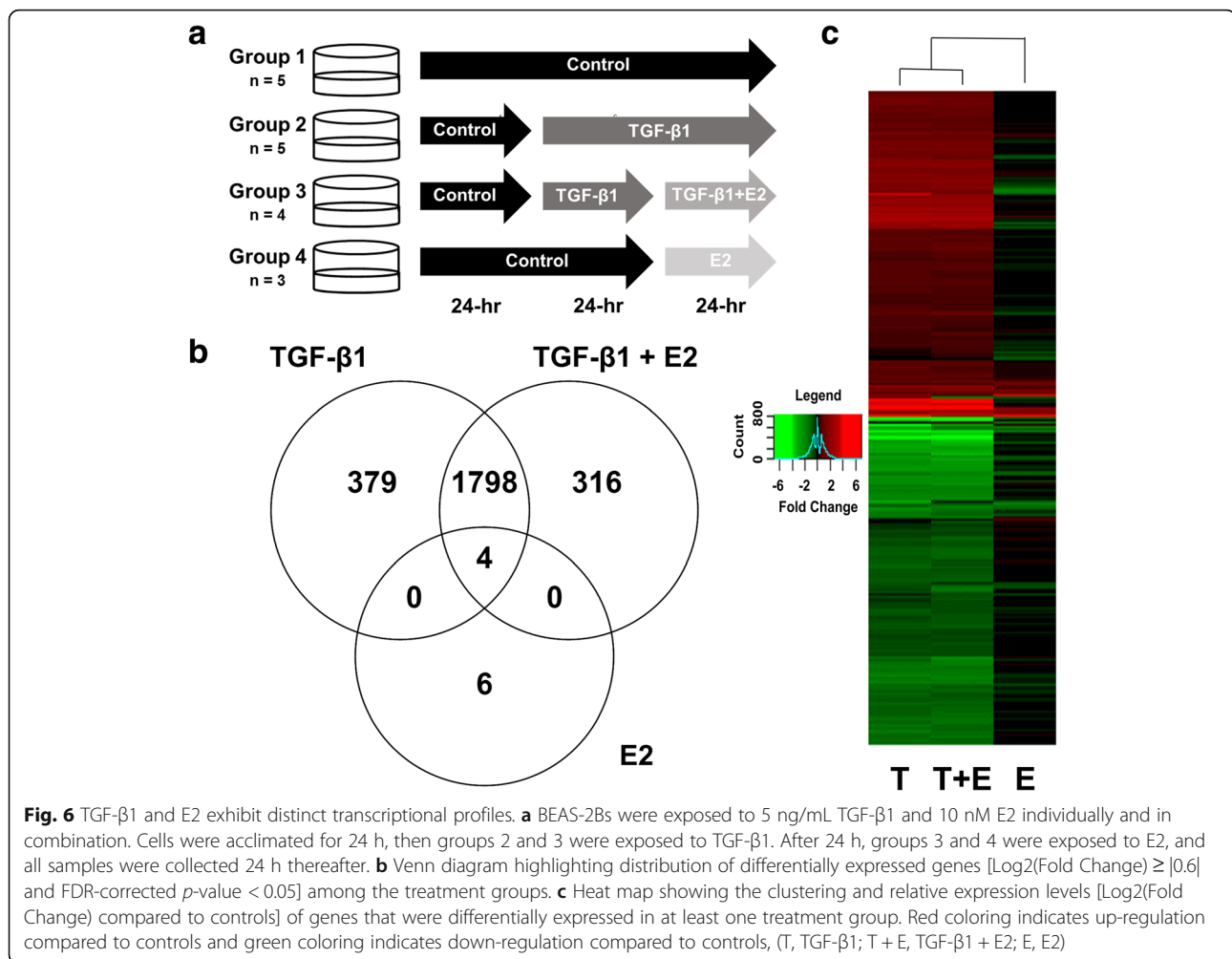


Fig. 6 TGF-β1 and E2 exhibit distinct transcriptional profiles. **a** BEAS-2Bs were exposed to 5 ng/mL TGF-β1 and 10 nM E2 individually and in combination. Cells were acclimated for 24 h, then groups 2 and 3 were exposed to TGF-β1. After 24 h, groups 3 and 4 were exposed to E2, and all samples were collected 24 h thereafter. **b** Venn diagram highlighting distribution of differentially expressed genes [Log₂(Fold Change) ≥ |0.6| and FDR-corrected *p*-value < 0.05] among the treatment groups. **c** Heat map showing the clustering and relative expression levels [Log₂(Fold Change) compared to controls] of genes that were differentially expressed in at least one treatment group. Red coloring indicates up-regulation compared to controls and green coloring indicates down-regulation compared to controls, (T, TGF-β1; T + E, TGF-β1 + E2; E, E2)

squamous cell lung tumors although a difference between *ESR1* and *ESR2* expression was not evident in normal lung cells [38]. These results are in contrast to a study by Mollerup et al. that found that *ESR2* was more abundantly expressed than *ESR1* [39] and another study by Couse et al. that found greater expression of *ESR2* in mouse lung [40]. The discrepancies may be a result of variable detection methods [38–40].

We probed a role for E2 in modulating TGF-β1-induced EMT because this process has been observed in fibrosis models although the relative contribution to fibrogenesis in humans is heavily debated [41–45]. TGF-β1 caused a significant reduction in expression of the epithelial cell type marker and a significant increase in expression of the mesenchymal cell type markers (Fig. 1b, d-f) similar to other studies [28–30]. Unlike the study by Doermer et al., we did not measure a significant increase in expression of *ACTA2* mRNA (Fig. 1c) which may be a result of the duration of exposure as this particular marker tends to be more highly induced at later time-points (5 days) [29] and is indicative of further

differentiation of fibroblasts into contractile myofibroblasts [46].

Using this model system, we determined whether E2 affected TGF-β1-induced EMT. A role for E2 in inhibiting EMT in humans was suggested in a study which found that reduced expression of *ESR1* was associated with increased expression of genes involved in EMT in endometrial carcinoma samples [47]. Further, EMT is a target for sex hormones in cell types such as breast and prostate cancer cells where E2 signaling maintains an epithelial phenotype and suppresses EMT [48–51]. In our analysis, exposure to E2 did not significantly affect EMT marker gene expression individually nor did it impact the normal TGF-β1 response (Fig. 2a-f). Co-exposure to TGF-β1 and E2 resulted in a trend of increased expression of *VIM* and *ACTA2* compared to TGF-β1 alone which is consistent with one study that reported E2 promoted reversible EMT-like transition and collective motility in breast cancer cells [52].

E2 may not affect TGF-β1-induced EMT due to direct actions of TGF-β1 on ESRs themselves. Interestingly, we

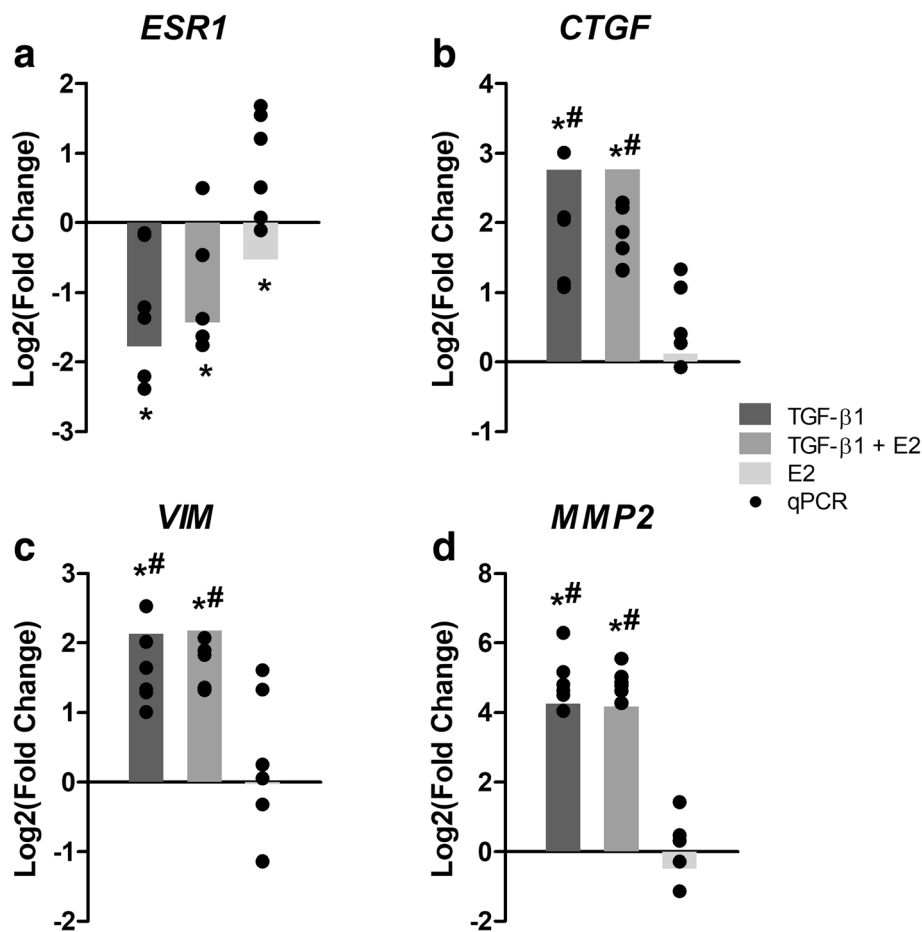


Fig. 7 Orthogonal validation of RNA-Seq data. **a-d** Expression of select genes was validated by qPCR; *ESR1* (**a**), Connective tissue growth factor (*CTGF*, **b**), *VIM* (**c**), and Matrix metalloproteinase 2 (*MMP2*, **d**), in an identical and independent experiment. Bars represent expression [Log₂(Fold Change)] of each gene in the RNA-Seq analysis, and black dots represent expression [Log₂(Fold Change)] in each sample ($n = 6$) in the orthogonal experiment as determined by qPCR relative to vehicle control (DMSO). Target gene expression as measured by qPCR was normalized to *GAPDH* mRNA expression and quantified as fold change to control using the relative $\Delta\Delta C_q$ method. Asterisks (*) indicate differential expression compared to controls [Log₂(Fold Change) $\geq |0.6|$ and FDR-corrected p -value < 0.05] in the RNA-Seq analysis, and pound signs (#) indicate statistically significant ($p < 0.05$) differences compared to vehicle controls in the qPCR data as determined by one-way ANOVA and Newman-Keuls multiple comparison test

Table 3 Genes differentially regulated by E2

ENSEMBL Gene ID	Gene	Description	Log ₂ (Fold Change)	p -value
ENSG00000258588	<i>TRIM6-TRIM34</i>	Tripartite Motif-Containing 6 And Tripartite Motif-Containing 34	5.36	1.33E-06
ENSG00000256966	<i>RP11-613 M10.8</i>	AL513165.2	3.61	2.98E-02
ENSG00000274944	<i>RP5-864 K19.6</i>	AL139260.3	2.93	1.34E-14
ENSG00000255439	<i>RP11-196G11.1</i>	AC135050.2	1.43	9.12E-03
ENSG00000187678	<i>SPRY4</i>	sprouty RTK signaling antagonist 4	0.76	3.20E-05
ENSG00000139318	<i>DUSP6</i>	dual specificity phosphatase 6	0.75	2.25E-08
ENSG00000169583	<i>CLIC3</i>	chloride intracellular channel 3	-0.73	1.40E-06
ENSG00000053918	<i>KCNQ1</i>	potassium voltage-gated channel subfamily Q member 1	-0.86	4.87E-03
ENSG00000111344	<i>RASAL1</i>	RAS protein activator like 1	-1.34	1.79E-03
ENSG00000162444	<i>RBP7</i>	retinol binding protein 7	-1.65	3.08E-02

Table 4 Significantly enriched gene sets

Name	Pathway Type	TGF- β 1		TGF- β 1 + E2		E2	
		Median Change	<i>p</i> -value	Median Change	<i>p</i> -value	Median Change	<i>p</i> -value
Airway Smooth Muscle Cell Contraction	Diseases	1.14	4.72E-04	1.10	4.34E-03	-1.01	3.96E-02
Alveolar Epithelial Cell Dysfunction	Diseases	1.01	4.98E-02	-	-	-	-
Ca ²⁺ Flux Regulation	Biological Function	1.02	2.12E-07	1.06	1.40E-05	-1.00	5.48E-09
Complement Alternative Pathway	Biological Function	-1.63	3.17E-04	-1.49	2.64E-05	-1.11	1.36E-03
Complement Classical Pathway	Biological Function	-1.34	2.27E-04	-1.49	3.09E-05	-1.15	4.87E-04
Extracellular Matrix Turnover	Biological Function	1.55	2.26E-08	1.53	3.98E-07	-1.04	6.86E-04
Histone Acetylation	Biological Function	-	-	-	-	1.04	3.68E-02
Histone Phosphorylation	Biological Function	-	-	-	-	1.05	2.99E-05
Neutrophil Chemotaxis	Biological Function	1.09	1.27E-03	1.07	7.25E-03	-	-
NURF in Chromatin Remodeling	Biological Function	-	-	-	-	1.06	2.48E-02
Skin Fibrosis	Diseases	1.07	2.15E-02	1.06	1.64E-02	-	-
Vasodilation Activation	Biological Function	-	-	-	-	-1.00	3.34E-02

(-), not significantly enriched in specified exposure group

found that exposure to TGF- β 1 caused a dose-dependent and significant reduction in *ESR1*, *ESR2*, and *GPB1* mRNA expression (Fig. 3b-c). We extended this to show that TGF- β 1-induced repression of *ESR1* persisted at the protein level (Fig. 4a-b). Other studies have shown that TGF- β 1 reduces *ESR1* mRNA expression [53, 54] and *ESR1* protein expression [54, 55] in breast epithelial cancer cells and *ESR2* protein expression in prostate cancer cells [51], however this is the first study to show that TGF- β 1 reduced *ESR2* and *GPB1* mRNA expression and certainly the first to report any interaction between TGF- β 1 and ESRs in bronchial epithelial cells. In support of this interaction occurring in vivo, we observed reduced expression of *ESR1*, *ESR2*, and *GPB1* in lung tissue from patients with end-stage IPF compared to healthy control subjects (Fig. 5a-c). Although we do not have measurements of TGF- β 1 in our samples, others have shown increased serum TGF- β 1 levels in patients with IPF compared to healthy controls [36]. These results should be carefully interpreted given the small sample size and the absence of mechanistic information linking increased serum TGF- β 1 levels to *ESR1*, *ESR2*, and *GPB1* mRNA expression. Future studies should investigate which signaling mediators downstream of TGF- β 1, e.g. SMADs, CTGF, or SNAIL1, among others, are responsible for the observed repression.

Few studies to date have revealed a functional role for E2 in lung cells as measured by genes and pathways modulated downstream. Using RNA-Seq, we searched for enriched pathways in BEAS-2Bs exposed to E2 and TGF- β 1 individually, and in combination, to both identify points of convergence of E2 and TGF- β 1 signaling and to highlight novel E2 targets that may be susceptible to TGF- β 1-induced repression of ESRs. Sequencing data indicated greater regulation of genes in response to TGF- β 1 exposure in comparison to

E2 exposure, perhaps consistent with the well-recognized strong pro-fibrotic response associated with TGF- β 1. Although some genes were differentially regulated in the TGF- β 1 or TGF- β 1 + E2 exposure groups, most were shared suggesting that the presence of E2 had a minimal effect on the TGF- β 1-induced transcriptome (Fig. 5b) potentially due to TGF- β 1-induced repression of ESRs. We confirmed the expression of selected genes relevant to this work and/or known to be targets of TGF- β 1 (Fig. 6, *ESR1*, *VIM*, *CTGF*, *MMP2*) which was consistent with our previous results and those reported in the literature [56–64].

Exposure to E2 did not induce as robust a transcriptional response in BEAS-2Bs compared to TGF- β 1. However, we identified statistically significant regulation of 10 genes by E2 (Table 3) that have not been previously reported. Two genes that were specifically down-regulated by E2 included Chloride intracellular channel 3 (*CLIC3*) and Retinol binding protein 7 (*RBP7*) (Table 3). *CLIC3* promotes migration and invasion of cancer cells by facilitating the functions of MT1-MMP (*MMP14*) [65, 66]. MT1-MMP is the most highly expressed MMP in IPF lungs [63] and may protect against PF by degrading collagen [67] and promoting lung repair [68]. Another study indicated that MT1-MMP promoted pulmonary fibrosis by activating latent TGF- β 1 [69]. Our results suggest E2 may repress MT1-MMP function by downregulating *CLIC3* mRNA expression. *RBP7*, also known as CRABP4, is a retinol binding protein thought to play an important role in retinol uptake, storage, and metabolism [70]. *RBP7* has been shown to be up-regulated in IPF lung tissue [71] and in wound tissue in the normal chicken chorioallantoic wound model [72] although its role in fibrosis is unclear. *RBP7* is positively regulated by E2 in breast cancer cells [73] and mouse mammary gland [74]. The discrepancy in regulation in our study may be a result of variable

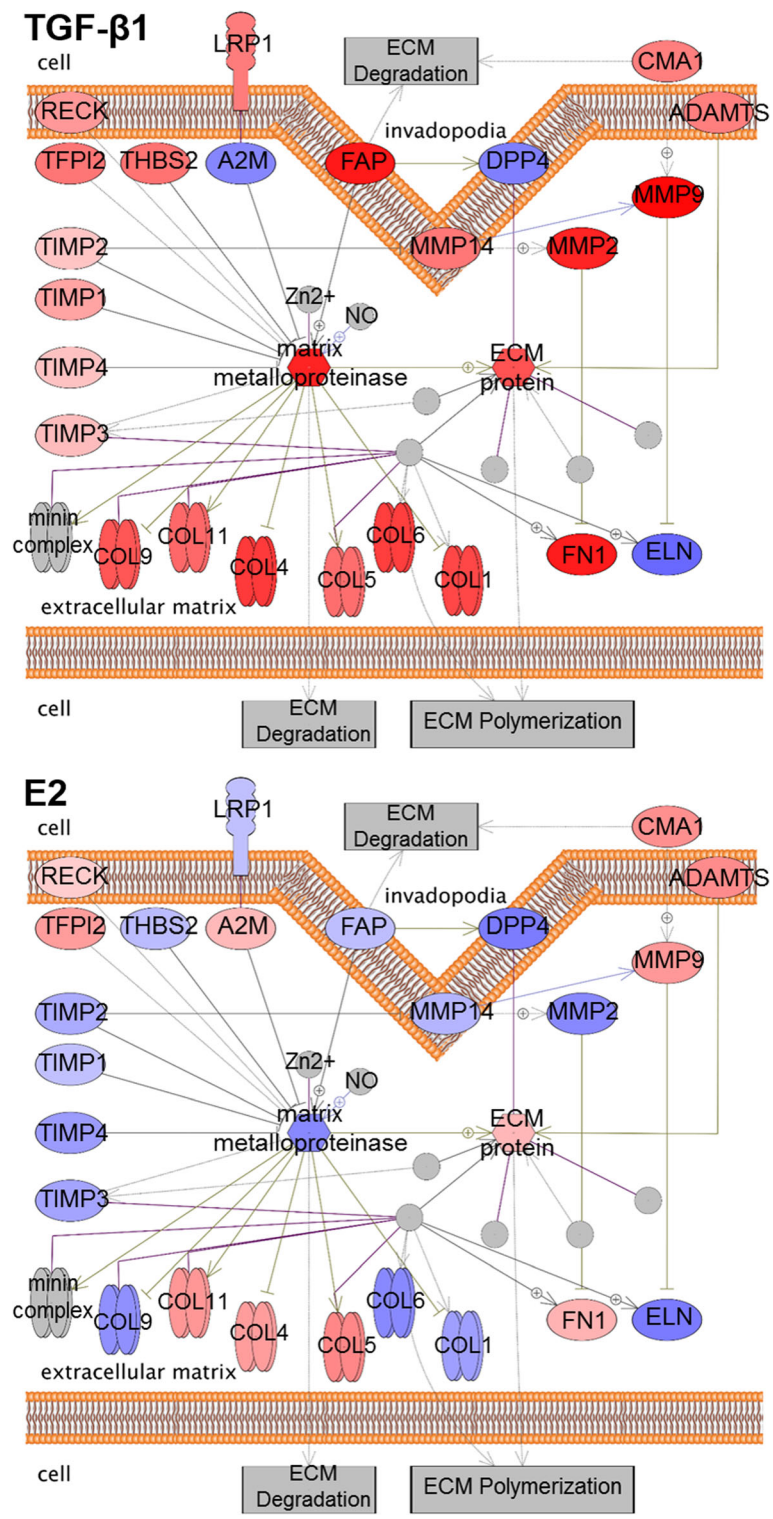


Fig. 8 TGF-β1 and E2 cause differential regulation of genes involved in extracellular matrix turnover. A gene set enrichment analysis using Pathway Studio of genes identified by RNA-Seq revealed that exposure to 5 ng/mL TGF-β1 (top) and 10 nM E2 (bottom) caused statistically significant ($p < 0.05$) enrichment of the extracellular matrix turnover pathway. Gray boxes denote cellular processes involved in the extracellular matrix turnover pathway. Red proteins indicate up-regulation and blue proteins indicate down-regulation as determined by RNA-Seq

exposure dynamics as the study by Calvo et al. exposed mice to one dose of E2 and sacrificed the animals 3 h later [74] while we exposed cells in vitro for 24 h. Nonetheless, E2 appears to regulate *RBP7* which may exhibit an unexplored effect on fibrogenic signaling.

As expected, exposure to TGF- β 1 resulted in significant enrichment of the ECM turnover (Fig. 8a), alveolar epithelial cell dysfunction, and skin fibrosis pathways as determined by GSEA (Table 4). It is well known that TGF- β 1 is involved in organization of the ECM [75] and neutrophil chemotaxis [76], and one of the prevailing hypotheses in IPF research is that it is a result of dysfunctional behavior of alveolar epithelial cells [77]. In this case, skin fibrosis serves as a surrogate for pulmonary fibrosis because the underlying mechanisms are similar and largely regulated by TGF- β 1 [78], and pulmonary fibrosis does not exist as a curated, predefined pathway in Pathway Studio. In most cases, pathways enriched in the TGF- β 1 individual exposure group were also enriched in the TGF- β 1 + E2 co-exposure group, and the overall directionality as indicated by the median change was similar. This suggests that E2 has a limited effect on TGF- β 1 once the pathways are in motion and/or was a result of TGF- β 1-induced repression of ESRs thus mirroring the results seen at the gene level (Fig. 3b-c).

Interestingly, exposure to E2 resulted in specific enrichment of multiple pathways involved in epigenetic regulation of chromatin structure and organization including Histone Acetylation, Histone Phosphorylation, and NURF in Chromatin Remodeling (Table 4). While E2 has been shown to regulate histone acetylation in A549 cells [79], little is known about a role for E2 in transcriptionally regulating the expression of genes involved in chromatin remodeling in the lung. This is important because evidence for the importance of epigenetics and chromatin organization in lung disease is growing, particularly in the context of pulmonary fibrosis [80–85]. For example, histone deacetylases are involved in activation of lung fibroblasts to myofibroblasts [86] and accumulation of ECM components and EMT in the diabetic kidney [87]. Notably, exposure to TGF- β 1 individually and in the presence of E2 did not result in enrichment of chromatin remodeling gene sets. This suggests that the absence of enrichment in the co-exposure group, despite the presence of E2, may be a result of TGF- β 1-induced repression of ESR expression and not through direct regulation of genes by TGF- β 1.

Similar to TGF- β 1, exposure to E2 resulted in statistical enrichment of genes associated with ECM turnover, airway smooth muscle cell contraction, and calcium flux regulation pathways (Table 4). E2 is known to influence the ECM in the uterus and vaginal tissues [88], in osteoblasts [89], and in the skin [90]. Interestingly, the overall directionality of the pathway as indicated by the median

change, was opposite (negative) compared to the directionality of the pathway in the TGF- β 1 and TGF- β 1 + E2 groups (positive, Table 4). This is consistent with a study that found that E2 inhibited TGF- β 1-induced ECM production in human and rat mesangial cells through GPER1 activation [22]. Of note is the repression of MMP14 and MMP2 as another study showed that E2 decreased MMP2-, MMP13-, and MMP14-mediated tissue matrix destruction [91]. These results are consistent with the significant reduction of *CLIC3* mRNA expression by E2 (Table 3) which is known to regulate MMP14 [65, 66]. Future studies should delineate the precise role of each ESR in regulating genes involved in ECM turnover.

Conclusions

In conclusion, we were not able to decipher an effect of E2 on TGF- β 1-induced EMT, but we do report the novel observation that TGF- β 1 inhibited *ESR1*, *ESR2*, and *GPER1* mRNA expression and ESR1 protein expression in BEAS-2Bs. We also report that E2 specifically down-regulated the expression of *CLIC3* and *RBP7* which have been associated with pathogenic mechanisms of pulmonary fibrosis. We further highlight cellular pathways involved in chromatin remodeling as novel and specific targets of E2 in bronchial epithelial cells and opposing actions of TGF- β 1 and E2 signaling on genes involved in ECM turnover. Although these data do not explicitly indicate a protective role for E2 in pulmonary fibrosis, these results suggest that E2 influences pathways relevant to pulmonary fibrosis and highlights potential roles for E2 in the lung that may contribute to sex-specific differences.

Additional file

Additional file 1: Table S1. Genes differentially expressed (FDR-corrected p -value < 0.05) in TGFB1 group compared to vehicle control group. **Table S2.** Genes differentially expressed (FDR-corrected p -value < 0.05) in TGFB1 + E2 group compared to vehicle control group. (XLS 479 kb)

Abbreviations

ACTA2: Alpha smooth muscle actin; ACTB: Beta-actin; BEAS-2Bs: Bronchial epithelial cells; CDH1: E-cadherin; CDH2: N-cadherin; CLIC3: Chloride intracellular channel 3; CRABP4: Cellular retinoic acid-binding protein 4; CTGF: Connective tissue growth factor; DMSO: Dimethyl sulfoxide; DUSP6: Dual specificity phosphatase 6; E2: 17 β -Estradiol; EMT: Epithelial to mesenchymal transition; ERCC: External RNA controls consortium; ESR: Estrogen receptor; ESR1: Estrogen receptor alpha; ESR2: Estrogen receptor beta; FN1: Fibronectin; FVC: Forced vital capacity; FVC%: Percent predicted forced vital capacity; GAPDH: Glycerinaldehyde phosphate dehydrogenase; GPER1: G-protein coupled estrogen receptor; GSEA: Gene set enrichment analysis; IPF: Idiopathic pulmonary fibrosis; KCNQ1: Potassium voltage-gated channel subfamily Q member 1; MIQE: Minimum information for publication of qPCR experiments; MMP14: Matrix metalloproteinase 14; MMP2: Matrix metalloproteinase 2; MT1-MMP: Matrix metalloproteinase 14; MT-MMP: Membrane-type matrix metalloproteinase; NURF: Nucleosome remodeling factor; PDGF: Platelet-derived growth factor; RASAL1: RAS protein activator like 1; RBP7: Retinol binding protein 7; RPS13: Ribosomal protein S13; SMAD3: SMAD family member 3; SNAIL1: Snail family transcriptional

repressor 1; SPRY4: Sprouty RTK signaling antagonist 4; TGF- β 1: Transforming growth factor beta1; UIP: Usual interstitial pneumonia; VIM: Vimentin

Acknowledgements

The authors would like to thank Yanping Zhang in the Gene Expression & Genotyping Core of the Interdisciplinary Center for Biotechnology Research (ICBR) for assistance with RNA-Seq library preparation, David Moraga of the NextGen DNA Sequencing core of UF ICBR for assistance with RNA sequencing, and Alberto Riva of the Bioinformatics core of UF ICBR for assistance with bioinformatics analysis of RNA-Seq data. The authors would also like to thank David Dreier and Amanda Buerger for assistance performing clustering analysis and creating heat maps.

Funding

This work was supported by funding from National Institutes of Health (R01HL114907 to T.S.A.). Research reported in this publication was supported by the UF Clinical and Translational Science Institute, which is supported in part by the NIH National Center for Advancing Translational Sciences under award number UL1TR001427. The content is solely the responsibility of the authors and does not necessarily represent the official views of the National Institutes of Health.

Availability of data and materials

The data discussed in this publication have been deposited in NCBI's Gene Expression Omnibus (39) and are accessible through GEO Series accession number GSE100574 (<https://www.ncbi.nlm.nih.gov/geo/query/acc.cgi?acc=GSE100574>).

Authors' contributions

LCS and TSA conceived the study and designed the experiments. LCS, SM, LR, KG, and SR performed the experiments. LCS and TSA interpreted the results. LCS drafted the manuscript and TSA edited. LCS, SM, LR, SR, AJB, and TSA approved the final version of the manuscript.

Ethics approval and consent to participate

The human lung tissue samples used in this study were a kind gift from Dr. Andrew Bryant. The deidentified, explanted lung tissue was obtained from subjects undergoing lung transplant for IPF and from lungs rejected for transplant from normal controls per the National Institutes of Health Lung Tissue Research Consortium (protocol no. 14-99-0011). The protocol for collection of lung tissue samples, and subsequent studies, were approved by the institutional review board at Vanderbilt University and the University of Florida (30).

Consent for publication

Not applicable.

Competing interests

The authors declare that they have no competing interests.

Publisher's Note

Springer Nature remains neutral with regard to jurisdictional claims in published maps and institutional affiliations.

Author details

¹Department of Physiological Sciences, University of Florida, Gainesville, FL, USA. ²Center for Environmental and Human Toxicology, University of Florida, Gainesville, FL, USA. ³Department of Environmental and Global Health, Center for Environmental and Human Toxicology, University of Florida, Box 110885, 2187 Mowry Rd, Gainesville, FL 32611, USA. ⁴Department of Medicine, University of Florida, Gainesville, FL, USA.

Received: 4 May 2018 Accepted: 13 August 2018

Published online: 30 August 2018

References

- Han MK, Murray S, Fell CD, Flaherty KR, Toews GB, Myers J, Colby TV, Travis WD, Kazerooni EA, Gross BH, Martinez FJ. Sex differences in physiological progression of idiopathic pulmonary fibrosis. *Eur Respir J*. 2008;31:1183–8.
- Gribbin J, Hubbard RB, Le Jeune I, Smith CJ, West J, Tata LJ. Incidence and mortality of idiopathic pulmonary fibrosis and sarcoidosis in the UK. *Thorax*. 2006;61:980–5.
- Olson AL, Swigris JJ, Lezotte DC, Norris JM, Wilson CG, Brown KK. Mortality from pulmonary fibrosis increased in the United States from 1992 to 2003. *Am J Respir Crit Care Med*. 2007;176:277–84.
- Raghu G, Weycker D, Edelsberg J, Bradford WZ, Oster G. Incidence and prevalence of idiopathic pulmonary fibrosis. *Am J Respir Crit Care Med*. 2006;174:810–6.
- Raghu G, Chen SY, Hou Q, Yeh WS, Collard HR. Incidence and prevalence of idiopathic pulmonary fibrosis in US adults 18–64 years old. *Eur Respir J*. 2016;48:179–86.
- McGee SP, Zhang H, Karmaus W, Sabo-Attwood T. Influence of sex and disease severity on gene expression profiles in individuals with idiopathic pulmonary fibrosis. *Int J Mol Epidemiol Genet*. 2014;5:71–86.
- Redente EF, Jacobsen KM, Solomon JJ, Lara AR, Faubel S, Keith RC, Henson PM, Downey GP, Riches DW. Age and sex dimorphisms contribute to the severity of bleomycin-induced lung injury and fibrosis. *Am J Physiol Lung Cell Mol Physiol*. 2011;301:L510–8.
- Voltz JW, Card JW, Carey MA, LM DG, Ferguson CD, Flake GP, Bonner JC, Korach KS, Zeldin DC. Male sex hormones exacerbate lung function impairment after bleomycin-induced pulmonary fibrosis. *Am J Respir Cell Mol Biol*. 2008;39:45–52.
- Valera IC, Kafaja S, Pham B, Fishbein M, Singh RR. Investigating mechanisms of sex bias in lung fibrosis using mice with sex chromosome complement. *J Immunol*. 2016;196:197–8.
- Gharaee-Kermani M, Hatano K, Nozaki Y, Phan SH. Gender-based differences in bleomycin-induced pulmonary fibrosis. *Am J Pathol*. 2005;166:1593–606.
- Haston CK, Wang M, Dejournett RE, Zhou X, Ni D, Gu X, King TM, Weil MM, Newman RA, Amos CI, Travis EL. Bleomycin hydrolase and a genetic locus within the MHC affect risk for pulmonary fibrosis in mice. *Hum Mol Genet*. 2002;11:1855–63.
- Lekgabe ED, Royce SG, Hewitson TD, MLK T, Zhao C, Moore XL, Tregear GW, Bathgate RA, Du XJ SCS. The effects of relaxin and estrogen deficiency on collagen deposition and hypertrophy of nonreproductive organs. *Endocrinology*. 2006;147:5575–83.
- Chang EC, Frasor J, Komm B, Katzenellenbogen BS. Impact of estrogen receptor β on gene networks regulated by estrogen receptor α in breast cancer cells. *Endocrinology*. 2006;147:4831–42.
- Ito I, Hanyu A, Wayama M, Goto N, Katsuno Y, Kawasaki S, Nakajima Y, Kajiro M, Komatsu Y, Fujimura A. Estrogen inhibits transforming growth factor β signaling by promoting Smad2/3 degradation. *J Biol Chem*. 2010;285:14747–55.
- Goto N, Hiyoshi H, Ito I, Tsuchiya M, Nakajima Y, Yanagisawa J. Estrogen and antiestrogens alter breast cancer invasiveness by modulating the transforming growth factor- β signaling pathway. *Cancer Sci*. 2011;102:1501–8.
- Ashcroft GS, Dodsworth J, Van Boxtel E, Tarnuzzer RW, Horan MA, Schultz GS, Ferguson MWJ. Estrogen accelerates cutaneous wound healing associated with an increase in TGF- β 1 levels. *Nat Med*. 1997;3:1209–15.
- Lovegrove AS, Sun J, Gould KA, Lubahn DB, Korach KS, Lane PH. Estrogen receptor α -mediated events promote sex-specific diabetic glomerular hypertrophy. *Am J Physiol Renal Physiol*. 2004;287:F586–91.
- Stope MB, Popp SL, Knabbe C, Buck MB. Estrogen receptor α attenuates transforming growth factor- β signaling in breast cancer cells independent from agonistic and antagonistic ligands. *Breast Cancer Res Treat*. 2010;120:357–67.
- Yamamoto T, Saatcioglu F, Matsuda T. Cross-talk between bone morphogenic proteins and estrogen receptor signaling. *Endocrinology*. 2002;143:2635–42.
- Matsuda T, Yamamoto T, Muraguchi A, Saatcioglu F. Cross-talk between transforming growth factor- β and estrogen receptor signaling through Smad3. *J Biol Chem*. 2001;276:42908–14.
- Kleuser B, Malek D, Gust R, Pertz HH, Potteck H. 17- β -estradiol inhibits transforming growth factor- β signaling and function in breast cancer cells via activation of extracellular signal-regulated kinase through the G protein-coupled receptor 30. *Mol Pharmacol*. 2008;74:1533–43.
- Li YC, Ding XS, Li HM, Zhang Y, Bao J. Role of G protein-coupled estrogen receptor 1 in modulating transforming growth factor- β stimulated mesangial cell extracellular matrix synthesis and migration. *Mol Cell Endocrinol*. 2014;391:50–9.
- Society AT. Idiopathic pulmonary fibrosis, diagnosis and treatment. (International consensus statement). *Am J Respir Crit Care Med*. 2000;161:646–64.

24. Travis WD, King TE, Bateman ED, Lynch DA, Capron F, Center D, Colby TV, Cordier JF, DuBois RM, Galvin J. American Thoracic Society/European Respiratory Society international multidisciplinary consensus classification of the idiopathic interstitial pneumonias. *Am J Respir Crit Care Med*. 2002;165:277–304.
25. Bryant AJ, Carrick RP, McConaha ME, Jones BR, Shay SD, Moore CS, Blackwell TR, Gladson S, Penner NL, Burman A. Endothelial HIF signaling regulates pulmonary fibrosis-associated pulmonary hypertension. *Am J Physiol Lung Cell Mol Physiol*. 2016;310:L249–62.
26. Smith LC, Ralston-Hooper KJ, Ferguson PL, Sabo-Attwood T. The G protein-coupled estrogen receptor agonist G-1 inhibits nuclear estrogen receptor activity and stimulates novel phosphoproteomic signatures. *Toxicol Sci*. 2016;151:434–46.
27. Smith LC, Clark JC, Bisesi JH, Ferguson PL, Sabo-Attwood T. Differential recruitment of co-regulatory proteins to the human estrogen receptor 1 in response to xenoestrogens. *Comp Biochem Physiol Part D Genomics Proteomics*. 2016;19:159–73.
28. Kamitani S, Yamauchi Y, Kawasaki S, Takami K, Takizawa H, Nagase T, Kohyama T. Simultaneous stimulation with TGF- β 1 and TNF- α induces epithelial mesenchymal transition in bronchial epithelial cells. *Int Arch Allergy Immunol*. 2011;155:119–28.
29. Doerner AM, Zuraw BL. TGF- β 1 induced epithelial to mesenchymal transition (EMT) in human bronchial epithelial cells is enhanced by IL-1 β but not abrogated by corticosteroids. *Respir Res*. 2009;10:100.
30. Hosper NA, van den Berg PP, de Rond S, Popa ER, Wilmer MJ, Masereeuw R, Bank RA. Epithelial-to-mesenchymal transition in fibrosis: collagen type I expression is highly upregulated after EMT, but does not contribute to collagen deposition. *Exp Cell Res*. 2013;319:3000–9.
31. Taylor S, Wakem M, Dijkman G, Alsarraj M, Nguyen M. A practical approach to RT-qPCR—publishing data that conform to the MIQE guidelines. *Methods*. 2010;50:S1–5.
32. Hellemans J, Mortier G, De Paepe A, Speleman F, Vandesompele J. qBase relative quantification framework and software for management and automated analysis of real-time quantitative PCR data. *Genome Biol*. 2007;8:R19.
33. Pfaffl MW. A new mathematical model for relative quantification in real-time RT-PCR. *Nucleic Acids Res*. 2001;29:e45.
34. Schneider CA, Rasband WS, Eliceiri KW. NIH Image to ImageJ: 25 years of image analysis. *Nature Methods*. 2012;9:671.
35. Edgar R, Domrachev M, Lash AE. Gene Expression Omnibus: NCBI gene expression and hybridization array data repository. *Nucleic Acids Res*. 2002;30:207–10.
36. Alhamad EH, Cal JG, Shakoor Z, Almogren A, AlBoukai AA. Cytokine gene polymorphisms and serum cytokine levels in patients with idiopathic pulmonary fibrosis. *BMC Med Genet*. 2013;14:66.
37. Subramanian A, Tamayo P, Mootha VK, Mukherjee S, Ebert BL, Gillette MA, Paulovich A, Pomeroy SL, Golub TR, Lander ES. Gene set enrichment analysis: a knowledge-based approach for interpreting genome-wide expression profiles. *Proc Natl Acad Sci USA*. 2005;102:15545–50.
38. Stabile LP, Davis ALG, Gubish CT, Hopkins TM, Luketich JD, Christie N, Finkelstein S, Siegfried JM. Human non-small cell lung tumors and cells derived from normal lung express both estrogen receptor α and β and show biological responses to estrogen. *Cancer Res*. 2002;62:2141–50.
39. Mollerup S, Jørgensen K, Berge G, Haugen A. Expression of estrogen receptors α and β in human lung tissue and cell lines. *Lung Cancer*. 2002;37:153–9.
40. Couse JF, Lindzey J, Grandien K, Gustafsson J, Korach KS. Tissue distribution and quantitative analysis of estrogen receptor- α (ER α) and estrogen receptor- β (ER β) messenger ribonucleic acid in the wild-type and ER α -knockout mouse. *Endocrinology*. 1997;138:4613–21.
41. Kim KK, Kugler MC, Wolters PJ, Robillard L, Galvez MG, Brumwell AN, Sheppard D, Chapman HA. Alveolar epithelial cell mesenchymal transition develops in vivo during pulmonary fibrosis and is regulated by the extracellular matrix. *Proc Natl Acad Sci USA*. 2006;103:13180–5.
42. Willis BC, Borok Z. TGF- β -induced EMT: mechanisms and implications for fibrotic lung disease. *Am J Physiol Lung Cell Mol Physiol*. 2007;293:L525–34.
43. Kage H, Borok Z. EMT and interstitial lung disease: a mysterious relationship. *Curr Opin Pulm Med*. 2012;18:517–23.
44. Bartis D, Mise N, Mahida RY, Eickelberg O, Thickett DR. Epithelial-mesenchymal transition in lung development and disease: does it exist and is it important? *Thorax*. 2014;69:760–5.
45. Kasai H, Allen JT, Mason RM, Kamimura T, Zhang Z. TGF- β 1 induces human alveolar epithelial to mesenchymal cell transition (EMT). *Respir Res*. 2005;6:56.
46. Kis K, Liu X, Hagood JS. Myofibroblast differentiation and survival in fibrotic disease. *Expert Rev Mol Med*. 2011;13:e27.
47. Wik E, Ræder MB, Krakstad C, Trovik J, Birkeland E, Hoivik EA, Mjos S, Werner HM, Mannelqvist M, Stefansson IM. Lack of estrogen receptor- α is associated with epithelial-mesenchymal transition and PI3K alterations in endometrial carcinoma. *Clin Cancer Res*. 2013;19:1094–105.
48. Dhasarathy A, Kajita M, Wade PA. The transcription factor snail mediates epithelial to mesenchymal transitions by repression of estrogen receptor- α . *Mol Endocrinol*. 2007;21:2907–18.
49. Guttilla IK, Adams BD, White BA. ER α , microRNAs, and the epithelial-mesenchymal transition in breast cancer. *Trends Endocrinol Metab*. 2012;23:73–82.
50. Ye Y, Xiao Y, Wang W, Yearsley K, Gao J, Shetuni B, Barsky S. ER α signaling through slug regulates E-cadherin and EMT. *Oncogene*. 2010;29:1451–62.
51. Mak P, Leav I, Pursell B, Bae D, Yang X, Taglienti CA, Gouvin LM, Sharma VM, Mercurio AM. ER β impedes prostate cancer EMT by destabilizing HIF-1 α and inhibiting VEGF-mediated snail nuclear localization: implications for Gleason grading. *Cancer Cell*. 2010;17:319–32.
52. Planas-Silva MD, Waltz PK. Estrogen promotes reversible epithelial-to-mesenchymal-like transition and collective motility in MCF-7 breast cancer cells. *J Steroid Biochem Mol Biol*. 2007;104:11–21.
53. Fridriksdottir AJ, Kim J, Villadsen R, Klitgaard MC, Hopkinson BM, Petersen OW, Rønnov-Jessen L. Propagation of oestrogen receptor-positive and oestrogen-responsive normal human breast cells in culture. *Nature communications*. 2015;6:8786.
54. Stoica A, Saceda M, Fakhro A, Solomon HB, Fenster BD, Martin MB. The role of transforming growth factor- β in the regulation of estrogen receptor expression in the MCF-7 breast cancer cell line. *Endocrinology*. 1997;138:1498–505.
55. Petrel TA, Bruggemeier RW. Increased proteasome-dependent degradation of estrogen receptor-alpha by TGF- β 1 in breast cancer cell lines. *J Cell Biochem*. 2003;88:181–90.
56. Sonnylal S, Xu S, Jones H, Tam A, Sreeram VR, Ponticos M, Norman J, Agrawal P, Abraham D, de Crombrughe B. Connective tissue growth factor causes EMT-like cell fate changes in vivo and in vitro. *J Cell Sci*. 2013;126:2164–75.
57. Leask A, Abraham DJ. The role of connective tissue growth factor, a multifunctional matricellular protein, in fibroblast biology. *Biochem Cell Biol*. 2003;81:355–63.
58. Mäkelä M, Larjava H, Pirilä E, Maisi P, Salo T, Sorsa T, Uitto V-J. Matrix metalloproteinase 2 (gelatinase A) is related to migration of keratinocytes. *Exp Cell Res*. 1999;251:67–78.
59. Kim ES, Sohn YW, Moon A. TGF- β -induced transcriptional activation of MMP-2 is mediated by activating transcription factor (ATF) 2 in human breast epithelial cells. *Cancer Lett*. 2007;252:147–56.
60. Seomun Y, Kim J, Choun-Ki J. Overexpression of matrix metalloproteinase-2 mediates phenotypic transformation of lens epithelial cells. *Biochem J*. 2001;358:41–8.
61. Kheradmand F, Rishi K, Werb Z. Signaling through the EGF receptor controls lung morphogenesis in part by regulating MT1-MMP-mediated activation of gelatinase A/MMP2. *J Cell Sci*. 2002;115:839–48.
62. Ravanti L, Kahari V. Matrix metalloproteinases in wound repair. *Int J Mol Med*. 2000;6:391–407.
63. García-Alvarez J, Ramirez R, Sampieri CL, Nuttall RQ, Edwards DR, Selman M, Pardo A. Membrane type-matrix metalloproteinases in idiopathic pulmonary fibrosis. *Sarcoidosis Vasc Diffuse Lung Dis*. 2006;23:13–21.
64. Craig VJ, Zhang L, Hagood JS, Owen CA. Matrix metalloproteinases as therapeutic targets for idiopathic pulmonary fibrosis. *Am J Respir Cell Mol Biol*. 2015;53:585–600.
65. Dozynkiewicz MA, Jamieson NB, MacPherson I, Grindlay J, van den Berghe PV, von Thun A, Morton JP, Gourley C, Timpson P, Nixon C. Rab25 and CLIC3 collaborate to promote integrin recycling from late endosomes/lysosomes and drive cancer progression. *Dev Cell*. 2014;127:3893–901.
66. Macpherson IR, Rainero E, Mitchell LE, Van Den Berghe PV, Speirs C, Dozynkiewicz MA, Chaudhary S, Kalna G, Edwards J, Timpson P. CLIC3 controls recycling of late endosomal MT1-MMP and dictates invasion and metastasis in breast cancer. *J Cell Sci*. 2014;127:3893–901.
67. Koenig GC, Rowe RG, Day SM, Sabeh F, Atkinson JJ, Cooke KR, Weiss SJ. MT1-MMP-dependent remodeling of cardiac extracellular matrix structure and function following myocardial infarction. *Am J Pathol*. 2012;180:1863–78.

68. Karow M, Popp T, Egea V, Ries C, Jochum M, Neth P. Wnt signalling in mouse mesenchymal stem cells: impact on proliferation, invasion and MMP expression. *J Cell Mol Med*. 2009;13:2506–20.
69. Mu D, Cambier S, Fjellbirkeland L, Baron JL, Munger JS, Kawakatsu H, Sheppard D, Broaddus VC, Nishimura SL. The integrin $\alpha v \beta 8$ mediates epithelial homeostasis through MT1-MMP-dependent activation of TGF- $\beta 1$. *J Cell Biol*. 2002;157:493–507.
70. Folli C, Calderone V, Ramazzina I, Zanotti G, Berni R. Ligand binding and structural analysis of a human putative cellular retinol-binding protein. *J Biol Chem*. 2002;277:41970–7.
71. Molyneux PL, Willis Owen SA, Cox MJ, James P, Cowman S, Loebinger M, Blanchard A, Edwards LM, Stock C, Daccord C. Host-microbial interactions in idiopathic pulmonary fibrosis. *Am J Respir Crit Care Med*. 2017;195(12):1640–50.
72. Soulet F, Kilarski WW, Antczak P, Herbert J, Bicknell R, Falciani F, Bikfalvi A. Gene signatures in wound tissue as evidenced by molecular profiling in the chick embryo model. *BMC Genomics*. 2010;11:495.
73. Kinyamu HK, Collins JB, Grissom SF, Hebbard PB, Archer TK. Genome wide transcriptional profiling in breast cancer cells reveals distinct changes in hormone receptor target genes and chromatin modifying enzymes after proteasome inhibition. *Mol Carcinog*. 2008;47:845–85.
74. Calvo E, Belleau P, Martel C, Labrie F. Specific transcriptional response of four blockers of estrogen receptors on estradiol-modulated genes in the mouse mammary gland. *Breast Cancer Res Treat*. 2012;134:625–47.
75. Blobe GC, Schiemann WP, Lodish HF. Role of transforming growth factor β in human disease. *New Engl J Med*. 2000;342:1350–8.
76. Parekh T, Saxena B, Reibman J, Cronstein BN, Gold LI. Neutrophil chemotaxis in response to TGF-beta isoforms (TGF-beta 1, TGF-beta 2, TGF-beta 3) is mediated by fibronectin. *J Immunol*. 1994;152:2456–66.
77. Fernandez IE, Eickelberg O. The impact of TGF- β on lung fibrosis: from targeting to biomarkers. *Proc Am Thorac Soc*. 2012;9:111–6.
78. Border WA, Noble NA. Transforming growth factor β in tissue fibrosis. *New Engl J Med*. 1994;331:1286–92.
79. Lai J-C, Cheng Y-W, Chiou H-L, Wu M-F, Chen C-Y, Lee H. Gender difference in estrogen receptor alpha promoter hypermethylation and its prognostic value in non-small cell lung cancer. *Int J Cancer*. 2005;117:974–80.
80. Coward WR, Saini G, Jenkins G. The pathogenesis of idiopathic pulmonary fibrosis. *Ther Adv Respir Dis*. 2010;4:367–88.
81. Coward WR, Watts K, Feghali-Bostwick CA, Jenkins G, Pang L. Repression of IP-10 by interactions between histone deacetylation and hypermethylation in idiopathic pulmonary fibrosis. *Mol Cell Biol*. 2010;30:2874–86.
82. Coward WR, Watts K, Feghali-Bostwick CA, Knox A, Pang L. Defective histone acetylation is responsible for the diminished expression of cyclooxygenase 2 in idiopathic pulmonary fibrosis. *Mol Cell Biol*. 2009;29:4325–39.
83. Rabinovich EI, Kapetanaki MG, Steinfeld I, Gibson KF, Pandit KV, Yu G, Yakhini Z, Kaminski N. Global methylation patterns in idiopathic pulmonary fibrosis. *PLoS One*. 2012;7:e33770.
84. Sanders YY, Ambalavanan N, Halloran B, Zhang X, Liu H, Crossman DK, Bray M, Zhang K, Thannickal VJ, Hagoood JS. Altered DNA methylation profile in idiopathic pulmonary fibrosis. *Am J Respir Crit Care Med*. 2012;186:525–35.
85. Yang IV, Schwartz DA. Epigenetics of idiopathic pulmonary fibrosis. *Transl Res*. 2014;165.1(2015):48–60.
86. Wang Z, Chen C, Finger S, Jung M, Schwarz H, Swanson N, Lareu R, Raghunath M. Suberoylanilide hydroxamic acid: a potential epigenetic therapeutic agent for lung fibrosis? *Eur Respir J*. 2009;34:145–55.
87. Noh H, Oh EY, Seo JY, Yu MR, Kim YO, Ha H, Lee HB. Histone deacetylase-2 is a key regulator of diabetes-and transforming growth factor- $\beta 1$ -induced renal injury. *Am J Physiol Renal Physiol*. 2009;297:F729–39.
88. Cox DA, Helvering LM. Extracellular matrix integrity: a possible mechanism for differential clinical effects among selective estrogen receptor modulators and estrogens? *Mol Cell Endocrinol*. 2006;247:53–9.
89. Komm BS, Terpening CM, Benz DJ, Graeme KA, Gallegos A. Estrogen binding, receptor mRNA, and biologic response in osteoblast-like osteosarcoma cells. *Science*. 1988;241:81.
90. Son ED, Lee JY, Lee S, Kim MS, Lee BG, Chang IS, Chung JH. Topical application of 17 β -estradiol increases extracellular matrix protein synthesis by stimulating TGF- β signaling in aged human skin in vivo. *J Invest Dermatol*. 2005;124:1149–61.
91. Pincus DJ, Kassira N, Gombosh M, Berho M, Glassberg M, Karl M, Elliot SJ, Thaller S. 17 β -Estradiol modifies diabetic wound healing by decreasing matrix metalloproteinase activity. *Wounds*. 2010;22:171–8.
92. Beck LA, Tancowny B, Brummet ME, Asaki SY, Curry SL, Penno MB, Foster M, Bahl A, Stellato C. Functional analysis of the chemokine receptor CCR3 on airway epithelial cells. *J Immunol*. 2006;177:3344–54.
93. Spizzo R, Nicoloso M, Lupini L, Lu Y, Fogarty J, Rossi S, Zagatti B, Fabbri M, Veronese A, Liu X. miR-145 participates with TP53 in a death-promoting regulatory loop and targets estrogen receptor- α in human breast cancer cells. *Cell Death Differ*. 2010;17:246–54.
94. Ye J, Coulouris G, Zaretskaya I, Cutcutache I, Rozen S, Madden TL. Primer-BLAST: a tool to design target-specific primers for polymerase chain reaction. *BMC Bioinformatics*. 2012;13:134.
95. Tanaka KI, Tanaka Y, Namba T, Azuma A, Mizushima T. Heat shock protein 70 protects against bleomycin-induced pulmonary fibrosis in mice. *Biochem Pharmacol*. 2010;80:920–31.
96. Untergasser A, Cutcutache I, Koressaar T, Ye J, Faircloth BC, Remm M, Rozen SG. Primer3—new capabilities and interfaces. *Nucleic Acids Res*. 2012;40:e115.
97. Nagaraja T, Chen L, Balasubramanian A, Groopman JE, Ghoshal K, Jacob ST, Leask A, Brigstock DR, Anand AR, Ganju RK. Activation of the connective tissue growth factor (CTGF)-transforming growth factor $\beta 1$ (TGF- $\beta 1$) axis in hepatitis C virus-expressing hepatocytes. *PLoS One*. 2012;7:e46526.

Ready to submit your research? Choose BMC and benefit from:

- fast, convenient online submission
- thorough peer review by experienced researchers in your field
- rapid publication on acceptance
- support for research data, including large and complex data types
- gold Open Access which fosters wider collaboration and increased citations
- maximum visibility for your research: over 100M website views per year

At BMC, research is always in progress.

Learn more biomedcentral.com/submissions

